20th Annual Conference of the Canadian Nuclear Society
Montreal, Quebec, Canada / May 30 - June 2, 1999

CHARACTERIZATION OF THE SLUG FORMATION IN COUNTER–CURRENT TWO–PHASE FLOWS

by:

TEYSSEDOU, A.[1] ONDER, N.,[1] SAYGIN, H.,[2]& HUYNG, H.[3]

[1] Institute of Nuclear Engineering,
Mechanical Engineering Department.
École Polytechnique de Montréal,

[2] Institute of Nuclear Engineering, Istanbul Technical University, Istanbul, Turkey.

[3] Nuclear Analysis Section, Hydro–Québec, Montréal.

1. INTRODUCTION

In CANDU reactors during a postulated Loss of Coolant Accident, the emergency cooling water coming from the inlet and outlet headers enters the fuel channels through the feeder pipes. These pipes consist of vertical and horizontal runs. In some feeders, orifices and/or venturi type flow obstructions are installed for flow adjustment and measurement. Steam produced in the feeders and/or in the fuel channels may flow in the direction opposite to that of the water, thereby creating vertical and horizontal counter–current two–phase flows (CCF) in the feeder pipes. Both vertical and vertical–to–inclined CCF phenomena have been extensively studied. It must be pointed out, however, that to the best of the authors' knowledge the slugging due to the interaction between an elbow and an orifice–type obstruction located in a horizontal pipe has not been studied yet. Further, even though the slugging phenomena in horizontal co–current flows have been extensively studied, among others by: Mishima & Ishii (1980), Kordyban & Ranov (1985) and Vanhout *et al.* (1992), the slug formation due to the interaction of an elbow and an orifice for horizontal CCF has never been treated. Thus, the aim of this paper is to present slugging data, i.e., slug frequency and propagation velocity, obtained under CCF conditions using a vertical–to–horizontal test section having orifices installed at different locations with respect to an elbow between vertical and horizontal legs.

2. THE EXPERIMENTAL FACILITY

The experimental facility used to carry out the experiments is shown in Figure 1. The test section has been manufactured of 63.5 mm I.D. transparent Plexiglas tubes. It consists of an upper and a lower plenum, and vertical and horizontal legs connected by an elbow. Flanges located at two axial positions in the horizontal leg are used to hold orifices having different sizes. The dimensions of the test section as well as the location of the flanges are shown in Figure 1. The orifices used for this work are made of 1.5 mm thick stainless steel plates without a chamfered edge. Orifices having β ratios ($= D_{orifice}/D_{tube}$) of 0.83, 0.77, 0.72 have been used for this research. Air and water under atmospheric pressure conditions are used as the working fluids. The water is supplied to the test section by a pump connected to a constant head tank. The temperature of the water is kept almost constant at $20\pm0.5°\,C$. The liquid is injected into the test section through a porous wall injector that consists of a tube having 800, 1 mm holes. The water is injected in the upper part of the test section just below the upper plenum (see Figure 1). Filtered air obtained from the mains of the laboratory is used as the gas phase. The air is injected through the lower plenum; care has been taken to avoid any interaction between the entrance of the air and the discharge of the test section in the lower plenum. The level of the water in the lower plenum is maintained constant by using a level controller manufactured at the IGN. This controller allows the level in the lower plenum to be controlled within ± 1 *cm* under all the transient flow conditions encountered during the experiments, i.e., onset of flooding, partial liquid delivery region and zero penetration point.

3. INSTRUMENTATION

The experimental facility is instrumented to measure liquid and gas flow rates, inlet flow temperatures, absolute pressures, and void fractions. The liquid flow rate is measured using "Flow Technology" turbine flow meters with an accuracy better than 1% of the reading. The gas flow rate is measured using a set of five "Brooks" rotameters with an accuracy of 2% of full scale. The temperature of the air is measured using a K–type thermocouple installed near the air entrance to the lower plenum. The absolute pressure in the lower plenum is measured using a 2 *psid* "Sensotec" pressure transducer with an accuracy of 0.25% of full scale. The void fraction measurement system, also used as the slug detection system consists of three mobile capacitance probes. The position of these probes (electrodes) is given in Figure 1. A schematic of this instrument is shown in Figure 2, it consists of mobile electrodes having a geometry that for void fractions lower than 70% allows an almost linear response to be obtained (Teyssedou & Tye, 1999). Each probe has its associated electronics module and anti–alias filters. Each module has been calibrated using a separate short test section (15 *cm*) having the same external diameter and wall thickness as the horizontal leg. The output of these modules are connected to a Data Acquisition System (DAS). The DAS is able of collecting 66000, 16–bits data points per run with a sampling time of 20 *ms*. This sampling time was selected after several trials in order to maximize the amount of data and to avoid aliasing of the signals. One of the channels of the DAS is used to read the signal produced by the pressure transducer located in the lower plenum.

4. EXPERIMENTAL PROCEDURES

For a given orifice size and position and a given inlet liquid flow rate the gas flow rate was increased until slugging was seen to occur. This procedure was then repeated for the entire partial liquid delivery region. For these experiments the entire range of partial liquid delivery was covered by changing the inlet liquid flow rate from 0.1 to 2.5 m^3/h. Fast Fourier Transform (FFT) and the Cross–Correlation techniques were used to treat the data. The Cross–Correlation of the signals produced by two consecutive void probes in conjuction with the distance between the probes is used to determine the slug propagation velocity.

5. EXPERIMENTAL RESULTS

In counter–current two–phase flows with orifices placed in the horizontal leg, the slug flow forms due to the interaction of waves triggered by a pulsating column that develops in the vertical leg and the partial reflections of these waves by the orifice (Tye, 1997). Figure 3 shows a typical void fraction record obtained with an orifice having a β ratio of 0.83 installed at position 1 in the horizontal leg (see Figure 1). It can be seen that for this particular case three slugs are formed at intervals of $\simeq 4\,s$. It is interesting to note that within the period occupied by the slugs, however, the void fraction is not able to reach 0%, i.e., test section completely filled with water. This is due to the fact that in some cases the slugs transport a non negligible amount of gas. The fluctuation of the void fraction observed in front of the slugs are caused by the large amplitude waves triggered by the pulsating column in the vertical leg that in the presence of an orifice behave as precursors to the slug formation. Moreover, the large accumulation of bubbles observed in front of the slugs is responsible for the sudden increase in void fraction that characterizes this region. After the passage of the slug the liquid film is considerably reduced. This is due to the fact that the slug behaves as an obstruction for the incoming liquid and that in this region most of the liquid is transported by the slug. This fact explains the high void fraction content measured within the slug tail region. It is also interesting to note the small amplitude, high frequency waves start appearing in this region. Figure 4 shows schematically a slug formed in the horizontal leg.

As mentioned above, the FFT was applied to the signals collected from the electrodes and the predominant frequency was determined from the maximum peak of the spectra. The best fits of predominant slug frequencies as a function of the gas superficial velocity obtained for the experiments carried out with orifices having the aforementioned β ratios installed at position 1 and position 2 in the horizontal leg, are presented in Figure 5. In general it is observed that for both positions and for all the orifices tested the frequency decreases with increasing superficial gas velocity. It can also be seen that for a given superficial gas velocity and for a given orifice β ratio the frequency of the slugs is much higher when the orifice is located closer to the elbow, i.e., position 1 in Figure 1. Furthermore, the predominant slugging frequencies are seen to increase with decreasing orifice β ratios. During the experiments it was observed that the slugs are formed by a constructive interference between waves that propagate in opposite directions. Large amplitude waves are generated by a pulsating column above the elbow. These waves travel along the horizontal leg and depending on the orifice size a partial reflection of the waves occurs at the orifice. The mutual interaction of the incident and the reflected waves brings about the bridging of the tube, i.e., formation of the slugs. This type of wave interaction can explain the fact that the predominant frequency decreases both with increasing superficial gas velocity and the size of the orifice. The increase in the superficial gas velocity increases the amount of entrained liquid thus, reducing the water level in the channel. In turn, the increase in the orifice size decreases the probability that the waves will be reflected. As the incident waves travel along the horizontal leg their amplitude gradually decreases, thus when the orifice is located farther from the elbow the probability of the incident and reflected waves of bridging the tube decreases, resulting in a lower slugging frequency.

The cross-correlation of the signals produced by two slug detection probes allowed the slug propagation velocity to be determined. The best fit of the slug propagation velocities as a function of the gas superficial velocity, obtained under the same conditions as described above is shown in the Figure 6. As observed for the slug frequency, the slug propagation velocity decreases with increasing superficial gas velocity. It is important to note, however, that the slug propagation velocity seems to be independent of the orifice β ratio as well as the position of the orifice with respect to the elbow. It is apparent that once the slugs are formed their propagation velocity must be controlled by kinematic conditions that are mostly dependent on the superficial gas velocity.

6. SLUG PROPAGATION VELOCITY MODEL

In order to predict the observed slug propagation velocities, a dynamic wave model as given in Wallis (1969) and Crowley et al. (1992) is adapted to handle counter–current two–phase flows. The model is developed by changing the frame of reference in such a way that the dynamic waves (slugs) are brought to rest. Thus, the new velocity field in the new frame of reference is written as follows:

$$U_k' = U_k - U_o \tag{1}$$

where $k = g$ or ℓ for the gas and the liquid phase respectively and U_o represent the slug propagation velocity. Using the new velocity field and assuming an incompressible flow, the mass and momentum conservation equations for an equivalent rectangular channel can be expressed as:

$$\frac{d}{dx}(U_k' h_k) = 0 \tag{2}$$

$$\rho_k U_k' \frac{dU_k'}{dx} = -\frac{dp}{dx} + f_k + b_k \, , \tag{3}$$

where h_k represents the space occupied by the k^{th} phase, the term f_k represents an interfacial drag force per unit volume and b_k the body forces per unit volume acting on the phases. Subtracting the liquid momentum conservation equation ($k = \ell$ in Eq. 3) from the gas momentum conservation equation ($k = g$ in Eq. 3), yields:

$$\rho_g U_g' \frac{dU_g'}{dx} - \rho_\ell U_\ell' \frac{dU_\ell'}{dx} = f_g - f_\ell + b_g - b_\ell \, . \tag{4}$$

Dynamic waves occurs when the right hand side of this equation depends linearly on the concentration gradients (Wallis, 1969) therefore, for slug flows it will depend on the heigh of the liquid phase, h. By neglecting the body forces acting on the phases ($b_k = 0$ in Eq. 3) this results in:

$$f_g - f_\ell = -(f_{\frac{\partial h}{\partial x}}) \frac{\partial h}{\partial x} \, . \tag{5}$$

Substituting this equation into Equation 4 after elimination of $\frac{dU_g'}{dx}$ and $\frac{dU_\ell'}{dx}$ by using the mass conservation equation for each phase and introducing the original velocities given by Equation 1, the slug propagation velocity can be written as:

$$U_o = \tilde{V} \pm \frac{\left(-\frac{\rho_g \rho_\ell \left(U_g - U_\ell\right)^2}{h(D-h)} - \left(\frac{\rho_g}{D-h} + \frac{\rho_\ell}{h} \right) f_{\partial h/\partial x} \right)^{1/2}}{\frac{\rho_g}{D-h} + \frac{\rho_\ell}{h}} . \tag{6}$$

The first term in this equation represents a weighted mean velocity which is not the same as the velocity of the center of mass and the second term represents a dynamic wave velocity, c, relative to the mean velocity $\tilde{V}$. It is apparent that in order to calculate the dynamic wave velocity from Equation 6, it is necessary to know the function $f_{\partial h/\partial x}$. This term is calculated from a balance of forces carried out in a volume containing the wave and takes the following form (Wallis, 1969):

$$f_g - f_\ell = (\rho_\ell - \rho_g) g\, h\, . \tag{7}$$

This equation in conjunction with Equation 6 are used to predict the slug propagation velocity. The values of h and $D - h$ are obtained from the time averaged void fractions as measured with the slug detection system. Furthermore, for a given inlet gas flow rate, i.e., gas superficial velocity, the velocity of the liquid phase is considered equal to the velocity of the entrained liquid phase. This velocity is calculated using the data of Bédard (1997).

The comparisons of the predictions of the model with the slug propagation velocity data obtained with orifices having β ratios of 0.72 and 0.77 located at position 1 and 2 in the horizontal leg are shown in Figure 7. As can be observed the predictions of the model are in excellent agreement with the data. In fact the predictions confirm that the slug propagation velocity decreases with increasing gas superficial velocity. It is important to mention however, that the model was not able to correctly predict the experimental trends observed for an orifice of $\beta = 0.83$. More work is still required to better analyze the data and determine the causes of this behavior. Further, it is apparent that in order to completely close the velocity calculations, additional work is still necessary to provide analytical tools capable of predicting the void fraction and the entrained liquid during the slug formation.

7. CONCLUSIONS

Preliminary results on the slugging phenomena in CCF carried out with a test section having vertical–to–horizontal legs, with different types of orifices installed at two locations in the horizontal leg have been presented. In general is observed that the predominant frequency of the slugs are affected by both the size and the position of the orifices with respect to the elbow. Possible explanations of these phenomena have been addressed. In addition, it is also observed that the slug propagation velocity is not affected by either the size of the orifice nor by the position of the orifice with respect to the elbow. It is important to point out that to the best of the authors' knowledge, this is the first attempt to carry out a study of slugging phenomena in CCF promoted by the interaction of an elbow with an orifice installed in a horizontal tube.

ACKNOWLEDGMENTS

This work was partially funded by the CANDU Owners Group, Working Party WPIR 1513.

References

[1] Barnea, D., Shoham, O., Taitel, Y. & Dukler, A.E.;"Flow pattern transition for gas-liquid flow in horizontal and inclined pipes," Int. J. Multiphase Flow 6,217-225 (1980).

[2] Bédard, S.; "Effet de la position d'une obstruction par rapport à un coude dans un écoulement diphasique contre–courant", Thèse de maîtrise, École Polytechnique de Montréal, (1997).

[3] Crowley, C.J.,Wallis, G.B., & Barry, J.J.; "Validation of a one–dimensional wave model for the stratified–to–slug flow regime transition, with consequences for wave growth and slug frequency," Int. J. Multiphase Flow 18, 249-271 (1992).

[4] Kordyban, E.S. & Ranov, T.; "Mechanism of slug formation in horizontal two–phase flow, "J. Bas. Engng Trans. ASME,92,857-864 (1970).

[5] Mishima, K. & Ishii, M.; "Theoretical Prediction of Onset of Horizontal Slug Flow," J. Fluids Engng., Vol. 102, pp. 441-445 (1980).

[6] Taitel, Y. & Dukler, A.E.; "A model for slug frequency during gas–liquid flow in horizontal and near–horizontal pipes, " Int. J. Multiphase Flow 3,585-596 (1977).

[7] Teyssedou, A. & P. Tye; "A slug detection system," Submitted to: Rev. Sci. Instrum., (Sept., 1998).

[8] Tye, P.; "Counter–current flow and flooding in vertical and horizontal tubes with and without obstructions," Ph.D. Thesis, École Polytechnique de Montréal (1997).

[9] Vanhout, R., Shemer, L. & Barnea, D.; "Spatial Distribution of Void Fraction within Liquid Slugs and other Related Slug Parameters," Int. J. Multiphase Flow, Vol, 18, pp. 831-845, (1992).

[10] Wallis, G.B.; "One–dimensional two–phase flow," McGraw–Hill, N.Y. (1969).

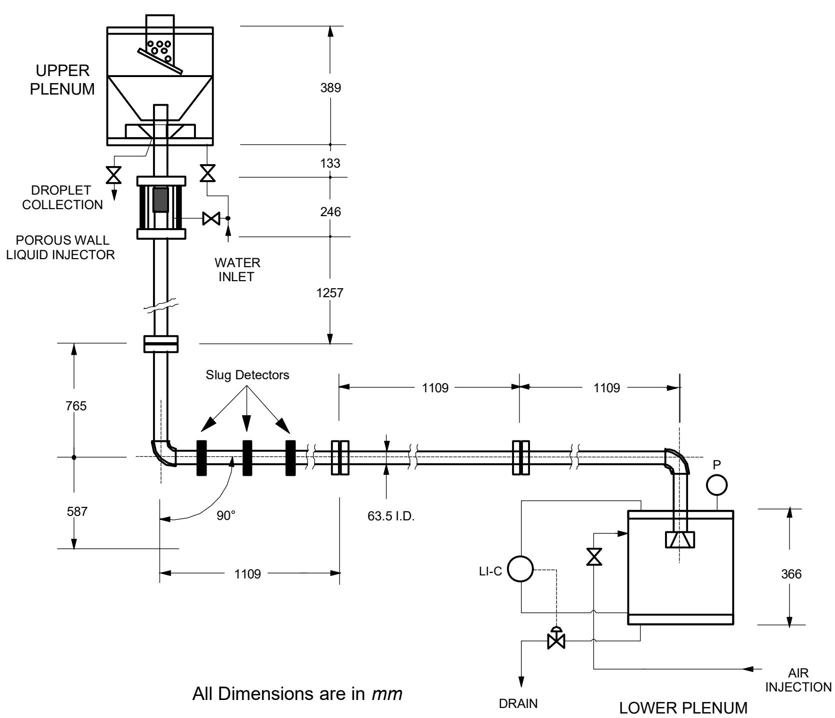

FIGURE 1. The Experimental Facility.

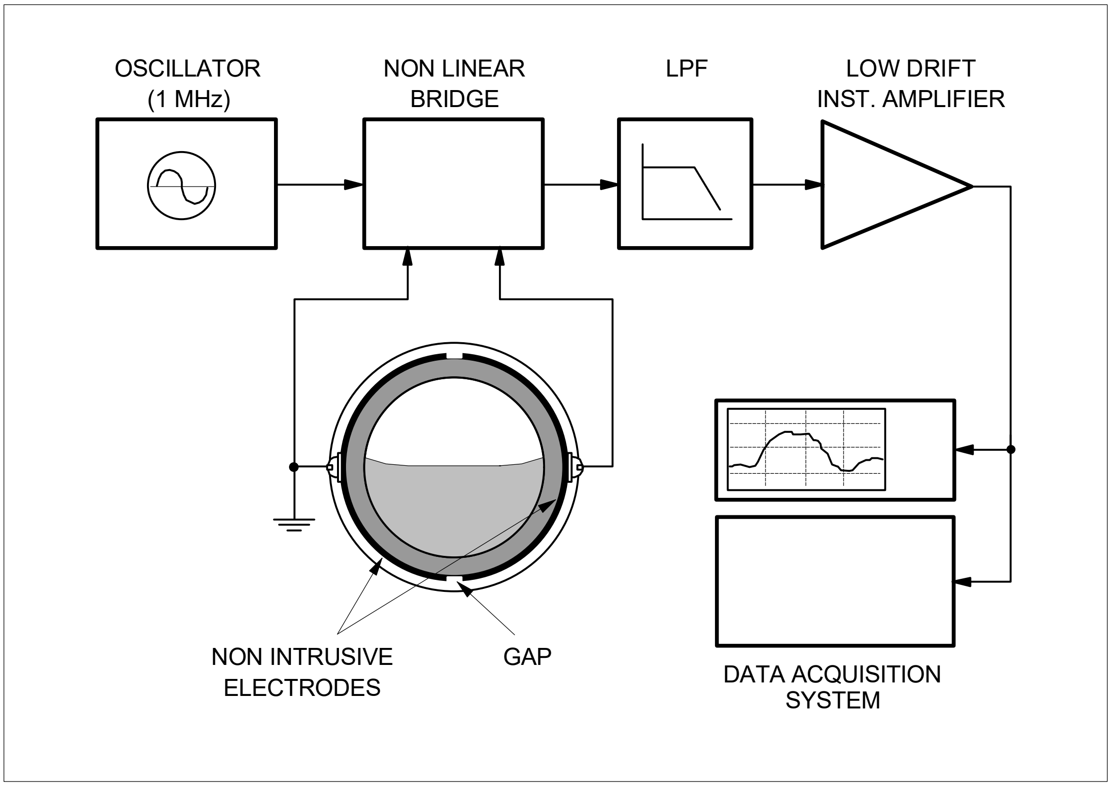

FIGURE 2. Schematic of the Slug Detection System.

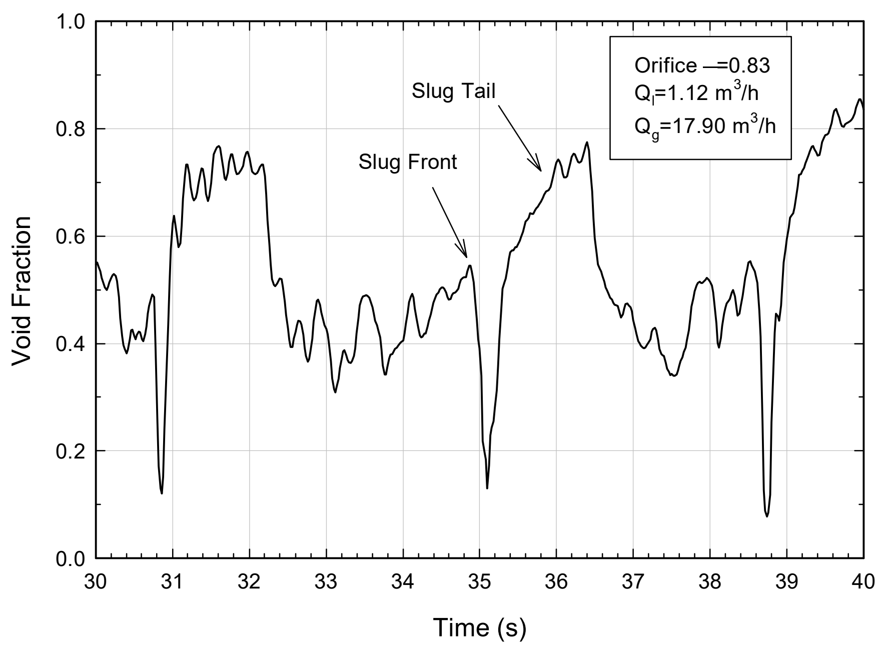

FIGURE 3. Typical Void Fraction Record.

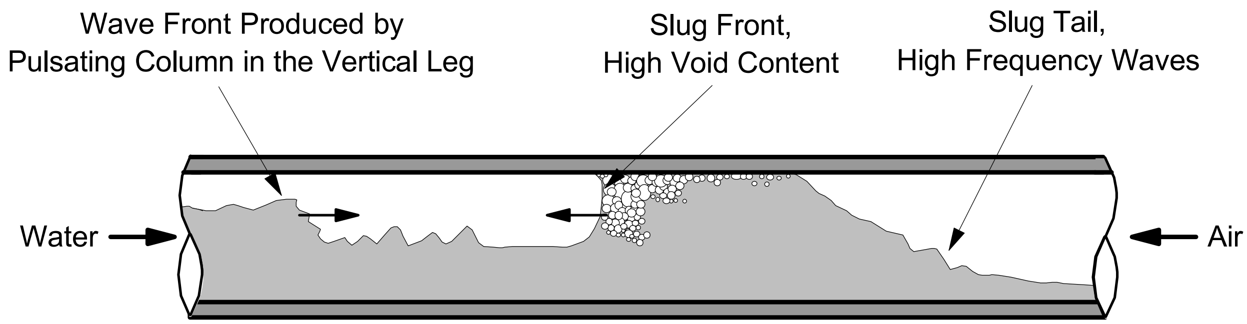

FIGURE 4. Slug Formed in the Horizontal Leg.

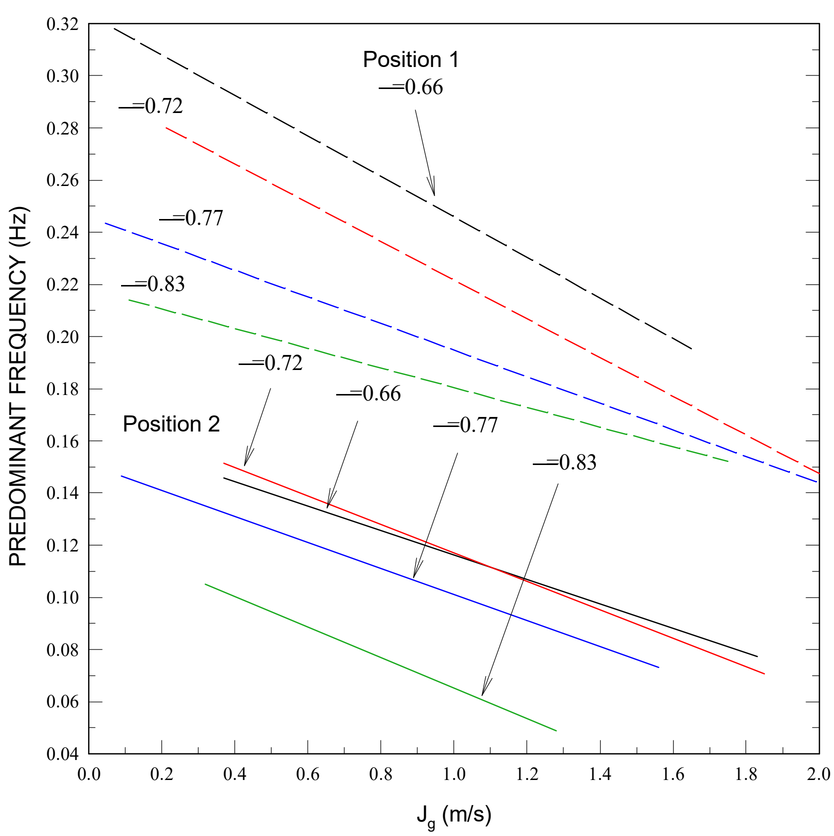

FIGURE 5. Predominant Frequency vs. Gas Superficial Velocity.

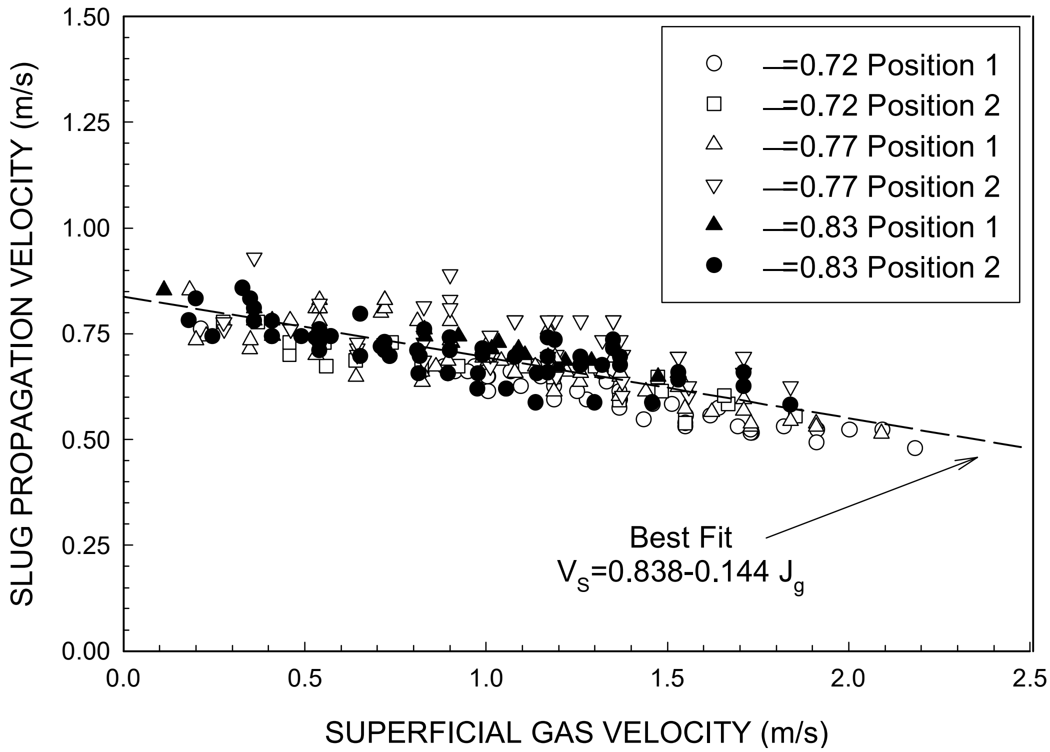

FIGURE 6. Slug Propagation Velocity vs. Gas Superficial Velocity.

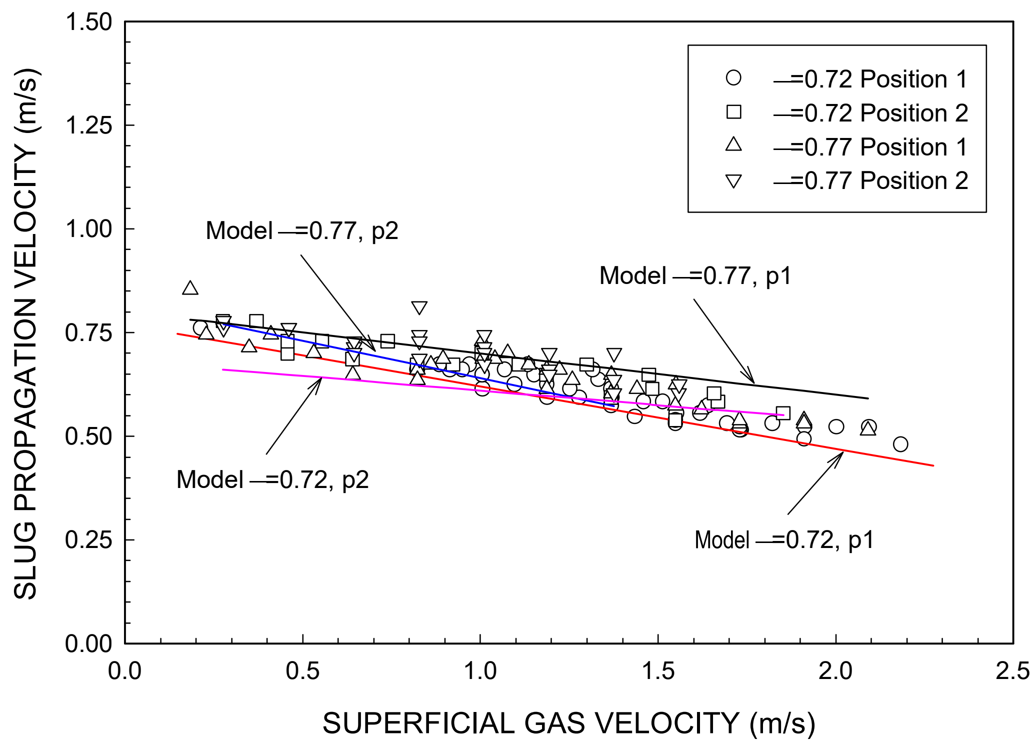

FIGURE 7. Comparison of the Predictions of the Model with Data.